Journal of the Nigerian Association of Mathematical Physics
***Volume28, No. 1,* (*November, 2014*), pp 223 – 234**
© J. of NAMP

Artificial Neural Networks Based Modelling for landslides susceptibility Zonation in a Part of Himalayas, India

***Levi I. Nwankwo* [1] *and Prashnant K. Champati-ray* [2]**

[1]Department of Physics, University of Ilorin, Ilorin 240003, Nigeria.
[2]Department of Geosciences, Indian Institute of Remote Sensing, Dehradun 248001

Abstract

Landslides are major natural geological hazards and each year these are responsible for enormous loss of human lives and property in Himalayan region spreading over Pakistan, India, Nepal, and Bhutan. Recent studies have revealed that landslides occur due to complex interaction of several geo-environmental parameters such as lithology, geological structures (faults, lineaments), geomorphology, slope gradient, slope aspect, soil texture, soil type, drainage, land use and anthropogenic factors. Attempts have been made to integrate such factors based on either statistical or heuristic approach to produce landslide hazard zonation maps showing relative susceptibility of a given area to landslide hazards. However, such methods have several limitations and therefore, an attempt is made to integrate layers by training the data set using artificial neural network (ANN) to arrive at more reliable results. The methodology was developed in an area within GiriValley in the Sirmour district of Himachal Pradesh, India. Causative parameters and landslide maps were derived from interpretation of satellite images, topographic maps, field survey and other maps. These parameters were taken into consideration while using the back-propagation of neural network method. The weights obtained from the trained network were consequently utilized for map integration and classification. The resulting landslide susceptibility zonation map delineates the area into five classes: Very High, High, Moderate, Low and Very Low. These classes were validated by correlating the results with actual landslide occurrences. The early results are very encouraging and attempts are being made to further improve the training and classification results.

1.0 Introduction

Landslides are major natural geological hazards and each year these are responsible for enormous loss of human lives and property in Himalayan region spreading over Pakistan, India, Nepal, and Bhutan. Recent studies have revealed that landslides occur due to complex interaction of several geo-environmental parameters such as lithology, geological structures, geomorphology, slope gradient, slope aspect, soil texture, soil type, drainage, land use and anthropogenic factors. Attempts have been made to integrate such factors based on either statistical or heuristic approach and produce landslide hazard zonation maps which shows the relative susceptibility of a given area to landslide hazards. However, such methods have several limitations and therefore, an attempt is made to integrate layers by training the data set using artificial neural network (ANN) to arrive at more reliable results. The motivation to use pattern recognition algorithms, such as artificial neural networks (ANNs), is to assist in the decision-making required in the assessment and mitigation of natural hazards. ANNs are computer models based loosely on the nonlinear neuronal structure of natural organisms. More properly, they are stimulus-response transfer functions, typically used to generalize an input-output mapping over a set of examples [1].

ANN techniques have been successfully applied in modelling and forecasting due to its flexibility and as a result, its use in the monitoring and assessment of landslides has received ample recent interest and quality of results [2 - 10]. For example, Pradhan *et al* [2] applied data mining model for landslide hazard mapping in Cameron Highland, Malaysia; Lee and Evangelista [3] mapped an earthquake induced susceptibility in Baguio City, Philippines using ANN, while Gomez and Kavzoglu [4] applied same in Jabonosa River Basin, Venezuela. These papers reported that ANNs offer a promising modelling alternative in landslide studies.

The purpose of this paper is therefore, to present a ANN modelling approach to landslide susceptibility mapping in a sampled area of the Himalayas. The study area is within GiriValley in the Sirmour district of Himachal Pradesh, India and bounded by latitudes 30^{o} 30’ N and 30^{o} 45’ N and longitudes 77^{o} 30’ E and 77^{o} 50’ E (Survey of India, 501,

Corresponding author:***Levi I. Nwankwo,***E-mail: levinwankwo@yahoo.com, Tel.: +2348034044244

topographic sheets 53 F/10). Mass movement is a common phenomenon in this area and during monsoons the population is often physically cut off from the external world for weeks. This causes many hardships for the people. In addition to natural causes, the slides in this area are also influenced by reckless mining activity [11]. The assessment of landslide hazard and the vulnerability of the population are particularly important for effective mitigation efforts in this area.

2.0 Artificial Neural Networks

Artificial Neural Networks (ANN) are a powerful mathematical learning technique composed of neurons, or processing elements, organized hierarchically in layers, which are able to emulate model components [12 - 14]. The concept of Artificial Neural Networks (ANN) and of course, artificial neurons were initially dealt with by McCulloch and Pitts [15], however, work on ANNs was relatively non-existent until the early 1980s, when Hopfield [16] set the stage for using ANNs in a wide array of multi-disciplinary fields. ANN models work to mimic the functions of biological neuron cells in the brain. A basic representation of the neuron and its interaction with other neurons is presented in Figure 1.

Communication of information among the brain's neurons is conducted through electrical pulses of various frequencies and magnitudes. These electrical pulses are produced as a response to the input of information into and within the body and allow communication not only within the brain but with all body functions (i.e., muscle response, organ function, etc.). The primary components of the neuron are the nucleus, dendrite, axon, and synapse. In general, dendrites are responsible for receiving information from other neurons, the axon sends an electrical signal (i.e., information) to neighbouring cells, and the synapse is the connection point between an axon on one cell and a dendrite from a neighbouring cell. Neurons function in a massively parallel manner as signal communications occur across many cells, and each cell can have as many as 10,000 dendrites that are continually being fed electrical signals. The many sources of signals being fed into an individual cell are resolved into a single signal, which is output through the axon and delivered to associated dendrite receptors.

ANN models retain some of the neurological vocabulary to describe the components of the system. The ANN model is therefore, comprised of three basic elements: A set of synapses (connecting links), each of which is characterized by a weight. The strength of the connection between an input and a neuron is noted by the value of the weight. Negative weight values reflect inhibitory connections, while positive values designate excitatory connections [17]. Secondly, an adder sums up all the inputs modified by their respective weights. This activity is referred to as linear combination and thirdly, an activation function which controls the amplitude of the output of the neuron. The neuronal model also includes an external bias which increases or lowers the net input of the activation function, depending whether it is positive or negative respectively.

Network architecture depicts the pattern of connections between neurons. Various network architectures are available. A single layered network typically consists of input units fully connected to the output units, whereas a multi-layered network (Figure 2) has one or more hidden layers in between. Various types of supervised ANNs also exist. A supervised ANN uses a training dataset for which both the input data and resulting output data are known. The supervision process defines relationships between input and output data by iteratively adjusting connection weights and reducing model errors. This adjustment occurs both at the individual neuron scale and globally through the model, attempting to reduce the model error over time. Back Propagation Neural Network (BPNN) multi-layered architecture with two hidden layers was used in this study. The first operation in a BPNN is the feed forward operation. During this operation, each input neuron receives an input signal and broadcasts this signal to the connected neurons Z_1, …, Zn in the first hidden layer. The total input to the Z_h neuron from the input layer is:

$$z(in)_h = \sum_{i=1}^{n} u_{ih} y_i + u_o h \qquad (1)$$

Each of these neurons then computes activation and sends its result to the connected neurons K_1, …, K_p in the second hidden layer. The total input to the K_j neuron from the first hidden layer is:

$$k(in)_j = \sum_{h=1}^{q} v_{jh} z_h + v_o j \qquad (2)$$

Each neuron in the second hidden layer computes its activation and sends its result to the output neuron. The total input to the output neuron O from the second hidden layer is:

$$O(in) = \sum_{j=1}^{p} k_j w_j + w_o \qquad (3)$$

Finally, the output neuron yields the network output according to the activation function O=f[O(in)]. The activation function is the same for all neurons in any particular layer of a neural network. In this work, the binary sigmoid function was utilized, which may have any value between plus and minus infinity and squashes the output into the range [0, 1]. The sigmoid function takes the form of:

$$f(x) = \frac{1}{1+e^{-x}} \qquad (4)$$

The backward pass is concerned with error computation and connection weight updates. The network output is compared with the target output to determine the error. An objective functions is defined as $E=0.5(t-o)^2$, and connection weights are updated using generalized delta rules. The update of the weights connecting the second hidden layer with the output equation (3) is given by:

$$w_{j,n} = w_{j,o} + \Delta w_j \qquad (5)$$

where $w_{j,n}$ and $w_{j,o}$ are new and old weights, respectively. The incremental weight is given by $\Delta w_j=-\mu\partial E/\partial w_j$, where μ is called the learning rate. Similar weight updates can be obtained for weights connecting the second and the first hidden layer, and the first hidden layer and the input layer.

3. 0 Data Base

Accurate detection of the location of landslides is very important for landslide susceptibility studies. Remote sensing products, such as satellite images and aerial photographs, could be used to obtain significant and cost-effective information on landslides. In this study, the thematic factors were derived from the interpretation of LANDSAT TM and SPOT PAN Images of the study area. The images were merged (Figure 3) for better spatial resolution and for the preparation of Landslide Inventory map. In addition, Survey of India topographic map (53f/10) at 1:50 000 scales (Figure 4) and geological map were also used. Extended field surveys were carried out in the study area to collect information on existing landslide distribution to assist in reliable creation of ANN data sets and validation of other thematic maps (Figure 5).

From the spatial database, landslide-related factors were calculated and extracted. The factors are lithology (derived from geology map), Land-use map (derived from topography map, aerial photo, satellite image and field investigation), drainage (derived from topography map), road map (topography map and satellite image), lineament (derived from topography map, aerial photo, satellite image and field investigation), slope amount and aspect (topography map), Mass wasting (satellite image and field investigation) and Vegetation (derived from satellite images). Using these nine factors, ANN methods were applied to analyze the landslide susceptibility. All the landslide inducing factors were converted to a raster grid of 10m x 10m cells, occupying 996 rows and 1 059 columns in all totalling 1 054 764 pixels with 33 265 cells of active landslides occurrences. However, for computation sake, the data was re-sampled to 199 rows and 211 columns in all totalling 41 989 pixels with 2 200 cells of active landslides occurrences using ILWIS 3.6 GIS software. The thematic data layer pertaining to each factor depicts the categories of each factor. Each category is assigned an attribute value, based on field survey and derived information values. These values depend upon their categories' relative significance in causing landslides. These attribute values subsequently were normalized to values ranging between 0 and 1 (1 denotes presence of landslide and 0 denotes absence), with respect to the highest attribute within the corresponding causative factor and for the input data for ANN. Table 1 shows the complete list of these input factors and their ratings considered in the ANN modelling.

4. 0 Neural Network Architecture and Implementation

The entire data set consist of 41 989 pixel points. Out of which 2 000 was used for training the network using the MATLAB software package. A framework of the neural network implementation used in this study is shown in Figure 6. The training data set consist of 1 000 pixels each for landslide and non landslides. 60% of the training vectors were used to train the network, while 20% was used to validate how well the network generalized. Training on the training vectors continues as long the training reduces the network's error on the validation vectors. After the network memorizes the training set (at the expense of generalizing more poorly), training is stopped. This technique automatically avoids the problem of over-fitting, which plagues many optimization and learning algorithms. Finally, the last 20% of the vectors provide an independent test of network generalization to data that the network has never seen. While training the dataset, the learning rate, number of epochs and root mean square error (RMSE) used for the stopping criterion were set to 0.01, 2 000 and 0.01 respectively. The 0.01 RMSE goal was met in most cases however, if the RMSE value was not achieved, then the maximum number of iterations was terminated at 2000.

The training dataset was used to train various networks by varying the number of neurons in both hidden layers, out of which the best 10 are present in Table 2**.** The input values for neural network processing corresponds to the attributes of the category of a thematic layer. After a classification algorithm such as ANN has been trained on data, the performance of the algorithm may be examined on specific training/test dataset. One common way of doing this would be to compute a gross measure of performance such as quadratic loss, accuracy, such as quadratic loss or accuracy, averaged over the entire test dataset. The classifier performance may also be watched more closely, for example, by plotting a Receiver Operating Characteristic (ROC) curve. A ROC curve shows true positive rate versus false positive rate (equivalently, sensitivity versus 1–specificity) for different thresholds of the classifier output. It can be used to find the threshold that maximizes the classification accuracy or to assess, in more broad terms, how the classifier performs in the regions of high sensitivity and high specificity, thereby analyzing the best performed architecture [1, 18, 19]. The performances of the networks are given in Table 2 and Figures 7 and 8. Based on the ROC analysis, the 9-17-3-1 structure was selected as the optimal architecture in this study. This architecture was found to adequately classify the training dataset with 94% accuracy and the whole data with 74% accuracy. It was not the highest classifier for the training dataset but it performed most optimally with the whole dataset. Moreover, care was taken to avoid over-fitting. Therefore, weights obtained from this network were subsequently used to obtain the network output of each pixel. The output values ranged from 0.012 to 0.998, which were categorized into six landslide susceptibility zones and used to produce the Landslide Susceptibility Zonation map (Figure 9).

Verifications were performed by comparing the forecast with existing landslide data (Figure 10), and the result is shown in Table 3. The ranges are classified into 5 classes, by area, the very low, low, moderate, high and very high zones has 13.92, 25.04, 28.26, 19.64 and 13.14 per cent of the total area respectively. The validation results show satisfactory agreement between susceptibility map and existing landslide location data. The ANN derived weights for the landslide-related factors and ranked accordingly is shown in Table 4 (The work by Kanungo *et al* [9] may be checked for details). Based of these ranking, the normalized weights obtained through the network at a scale from 0 to 10 for mass wasting, lithology, road zone, slope amount, vegetation, lineament, drainage, slope aspect and land-use are 2.32, 1.95, 1.40, 1.11, 0.91, 0.89, 0.67, 0.48 and 0.28 respectively. The higher the value of weight, the more crucial the factor is for the occurrence of landslides. Therefore, the network categorized mass wasting as rank 1, lithology as rank 2 and followed by other factors as presented above.

5.0 Conclusion

An artificial Neural Network approach to estimating the areas susceptible to landslides using a spatial database is presented. The analysis was applied in the GiriValley, Indian part of Himalayas. In the study area, landslide occurrence locations detected from satellite interpretation and field survey were formed into GIS database. From the spatial database, landslide-related factors were calculated and extracted. The factors are lithology (derived from geology map), Land-use map (derived from topography map, aerial photo, satellite image and field investigation), drainage (derived from topography map), road map (topography map and satellite image), lineament (derived from topography map, aerial photo, satellite image and field investigation), slope amount and aspect (topography map) and Vegetation (derived from satellite images). Using these nine factors, ANN methods were applied to analyze the landslide susceptibility. For application of the ANN, training sites were selected from landslide-related factors and a back-propagation algorithm was applied to calculate weights between input layers and hidden layer and between hidden layers and output layers by modifying the number of hidden layer. The weights were subsequently applied to the entire study area. The result of the analysis was used to construct a GIS layer, which was mapped and verified by correlating the observed data and landslide occurrence location. The result of the verification was in satisfactory agreement between the susceptibility map and the landslide location map. These early results are very encouraging and attempts are being made to further improve the training and classification results by employing ANN methods implemented using fuzzy based procedure.

6.0 Acknowledgements

The Centre for International Co-operation in Science (CICS), India is acknowledged for the Research Training Fellowship for Developing Country Scientists (RTFDCS) awarded to one of the authors. Indian Institute of Remote Sensing (IIRS) under the Indian Space Research Organization (ISRO) is also acknowledged for the facilities provided.

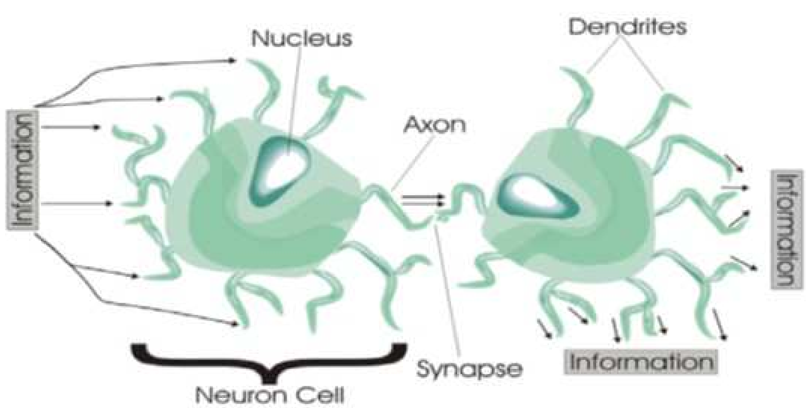

Figure 1:A simplified graphic representation of a neuron cell processing and transmitting information from cell to cell (adapted from [13]).

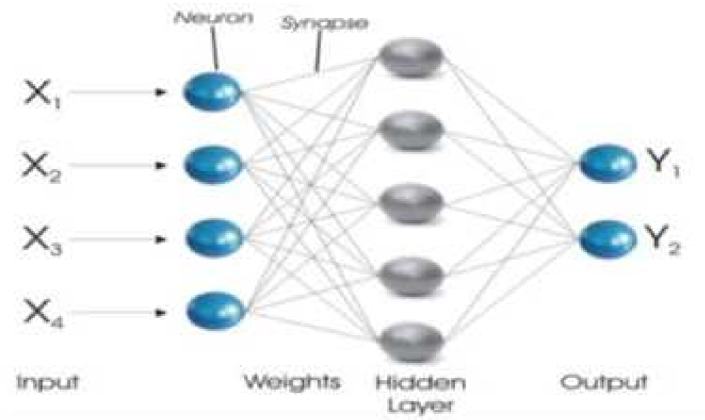

Figure 2:A common and simple ANN schematic that represents the flow of information from the input data, to the receipt of the input neurons, to weighting and evaluating of data, to signal adjustments in the hidden layer, and finally the resulting output data (adapted from [14]).

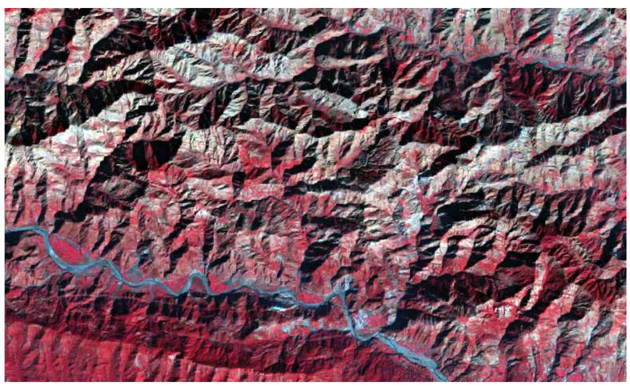

Figure 3:TM + SPOT PAN FCC 432 merged image of the study area.

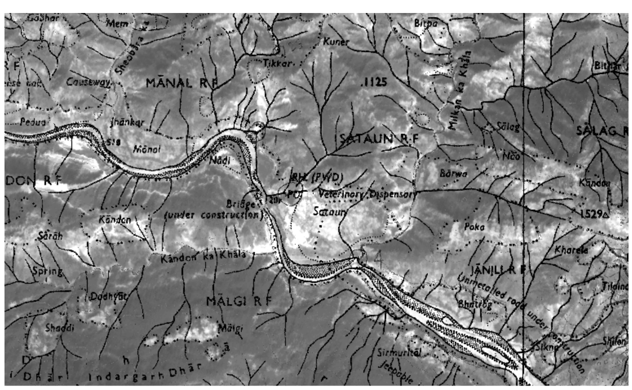

Figure 4: SPOT PAN with topographical details of the study area.

Figure 5: Some landslides in the study area.

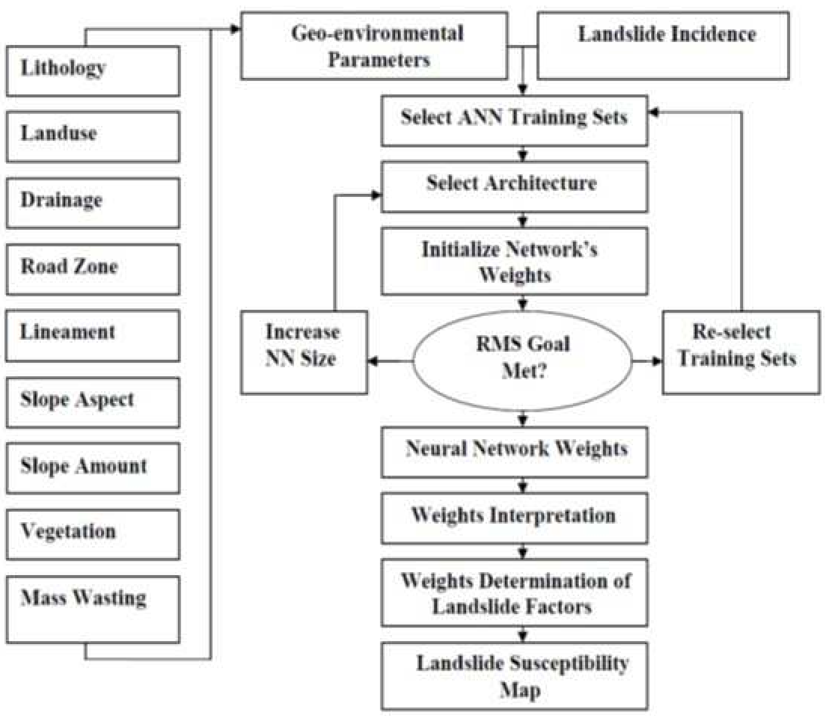

Figure 6: Flowchart showing the Methodology of ANN implementation used in the study.

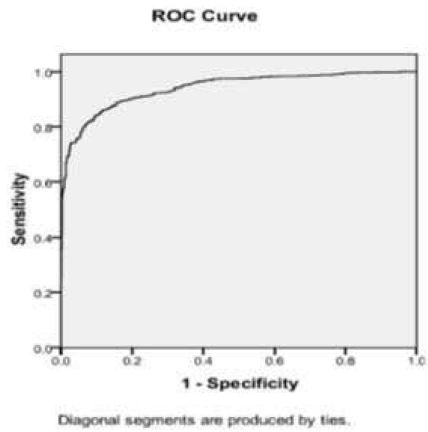

Area Under the Curve

Area	Std. Error[a]	Asymptotic Sig.[b]	Asymptotic 95% Confidence Interval	
			Lower Bound	Upper Bound
.940	.005	.000	.930	.950

The test result variable has at least one tie between the positive actual state group and the negative actual state group. Statistics may be biased.

a. Under the nonparametric assumption

b. Null hypothesis: true area = 0.5

Figure 7:ROC of the developed ANN model (9-17-3-1) on Training/Testing Data set

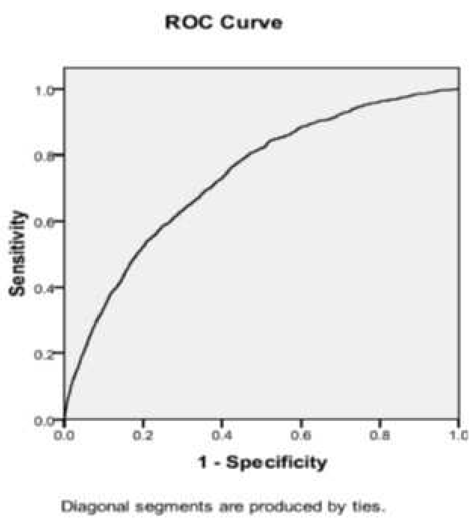

Area Under the Curve

Area	Std. Error[a]	Asymptotic Sig.[b]	Asymptotic 95% Confidence Interval	
			Lower Bound	Upper Bound
.734	.005	.000	.724	.744

The test result variable has at least one tie between the positive actual state group and the negative actual state group. Statistics may be biased.

a. Under the nonparametric assumption

b. Null hypothesis: true area = 0.5

Figure 8:ROC of the developed ANN model (9-17-3-1) on the entire Data set

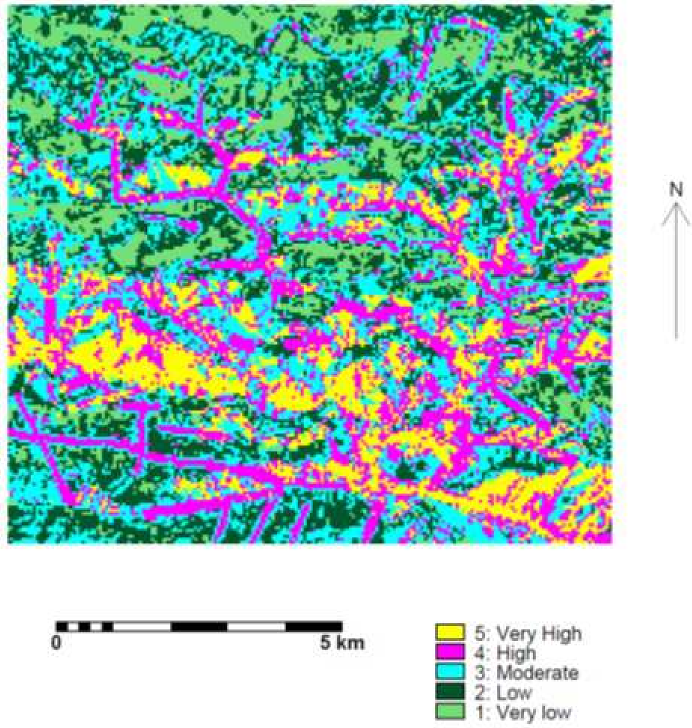

Figure 9: ANN modelled Landslide Susceptibility Zonation map of the study area.

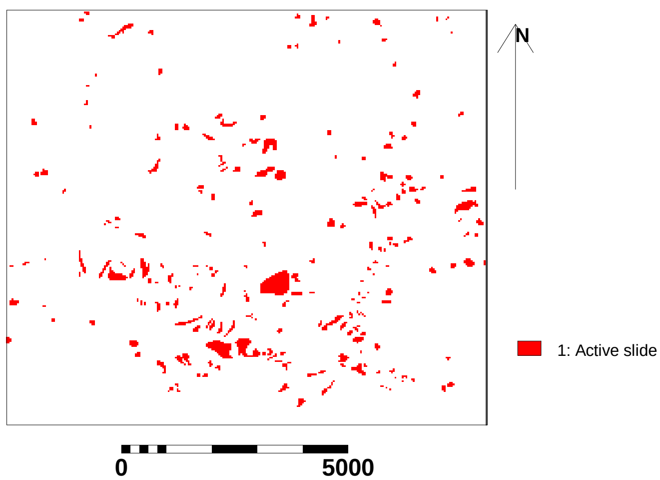

Figure 10: Landslide Incidence map of the study area.

Table 1. Normalized Ratings of causative factors

Causative Factors	Categories	Ratings	Normalized Ratings
Aspect	North	2	0.250
	Northeast	3	0.375
	East	5	0.625
	Southeast	6	0.750
	South	8	1.000
	Southwest	7	0.875
	West	4	0.500
	Northwest	1	0.125
Drainage	<50m	4	1.000
	50-75m	3	0.750
	Giri River	1	0.250
	>75m	2	0.500
Lineament	<50m	3	1.000
	50-100m	2	0.667
	>100m	1	0.337
Lithology	Basantpure Fm	5	0.417
	Blaini Fm	6	0.500
	Chandpur Fm	10	0.833
	Damta	12	1.000
	Deoban	11	0.917
	Krol A	4	0.333
	Krol B	9	0.75
	Krol CDE	3	0.250
	Lower Tal	1	0.083
	Siwalik Gr	2	0.167
	Subathu	7	0.583
	Up Tal	8	0.667
Landuse	Drainage	8	0.8
	River bed	4	0.4
	Agriculture	3	0.3
	Thin Vegetation	6	0.6
	Scrub land	7	0.7
	Slide like	10	1.0
	Forest 1	2	0.2
	Forest 2	1	0.1
	Quarry	9	0.9
	Barren area	5	0.5
Vegetation (NDVI)	Very Low	5	1.0
	Low	4	0.8
	Moderate	3	0.6
	High	2	0.4
	Very High	1	0.2
Mass wasting	Very High	3	1.000
	High	2	0.667
	Unclassified	1	0.333
Road Zone	<50m	3	1.000
	50-75m	2	0.667
	>75m	1	0.333
Slope Amount	<10	1	0.167
	11-20	2	0.333
	21-30	3	0.500
	31-40	4	0.667
	41-50	5	0.833
	>50	6	1.000

Table 2. ANN Architecture performance

(a). Training/testing data set

ANN Architecture	Performance (sse, rmse, msne)	ROC (%)
9-20-1	211.928, 0.106, 0.424	93.3
9-10-6-1	705.089, 0.353, 1.410	58.7
9-15-3-1	228.834, 0.114, 0.458	71.6
9-17-3-1	**188.839, 0.094, 0.378**	**94.0**
9-17-4-1	188.911, 0.945, 0.378	93.2
9-17-5-1	158.515, 0.079, 0.3170	95.6
9-17-6-1	242.347, 0.121, 0.485	90.1
9-17-8-1	107.385, 0.054, 0.218	96.7
9-18-4-1	192.791, 0.096, 0.386	92.9
9-18-5-1	170.699, 0.085, 0.341	94.8

sse – sum squared error, rmse – root mean square error, msne – mean square normalized error

(b). Entire data set

ANN Architecture	ROC (%)
9-20-1	71.6
9-10-6-1	52.4
9-15-3-1	66.9
9-17-3-1	**73.4**
9-17-4-1	69.2
9-17-5-1	70.7
9-17-6-1	67.3
9-17-8-1	66.9
9-18-4-1	71.1
9-18-5-1	71.3

Table 3. Comparison of landslide occurrence and landslide susceptibility map

Susceptibility Class	No. of cells	No. of cells (%)	No. of landslide occurred cells	No. of landslide occurred cells (%)
Very Low	5851	13.92	66	2.63
Low	10515	25.04	232	9.26
Moderate	11878	28.26	601	24.00
High	8255	19.64	662	26.43
Very High	5526	13.14	944	37.68
Total	41989	100.00	2505	100.00

Table 4. Process of ANN derived weights for thematic factors

A . INPUT LAYER (IL) - HIDDEN LAYER A (HLA) Connecting Weights

	HLA1	HLA2	HLA3	HLA4	HLA5	HLA6	HLA7	HLA8	HLA9	HLA10	HLA11	HLA12	HLA13	HLA14	HLA15	HLA16	HLA17
IL1	-0.229	-0.296	-0.196	-0.327	-0.958	0.378	-0.112	0.665	1.007	-0.492	0.645	0.541	0.692	-1.034	-1.106	-0.298	-0.426
IL2	-0.622	1.096	-0.496	0.204	-0.448	0.042	1.054	-0.729	-1.168	-0.423	1.455	-0.454	0.596	0.705	-0.209	1.020	-1.004
IL3	0.476	0.574	0.405	-0.078	-0.978	-0.770	0.351	0.599	0.656	-0.312	1.137	0.021	-0.809	0.215	-0.295	0.565	0.920
IL4	-0.603	1.586	0.681	-0.813	-0.854	0.950	0.096	0.869	1.077	-1.605	0.829	0.733	0.402	0.051	-0.080	-0.573	-0.783
IL5	-1.252	-0.377	-0.484	-0.120	-0.045	-0.483	1.483	0.842	0.624	-0.952	0.823	0.808	-0.535	0.881	-0.456	0.391	-0.153
IL6	0.399	-0.675	-0.467	-1.360	0.120	-1.171	0.097	-0.083	0.277	0.722	0.671	0.526	0.345	-0.123	-0.827	-0.485	0.244
IL7	0.234	-0.834	0.151	1.131	-0.480	-0.946	-0.889	0.069	1.171	-0.326	0.562	-0.500	0.207	0.194	0.097	0.985	-0.894
IL8	0.784	-0.650	-0.860	0.784	-0.463	-1.262	0.652	-0.128	0.378	-0.521	-0.971	0.499	0.020	-0.736	-0.323	-0.394	-0.040
IL9	-0.822	-0.143	0.794	0.342	0.545	-0.308	0.950	0.823	0.414	0.525	0.051	1.024	-1.113	0.041	-0.652	-0.376	-0.776

B. HIDDEN LAYER A (HLA)-HIDDEN LAYER B (HBL) Connecting Weights

	HLB1	HLB2	HLB3
HLA1	-0.268	-0.663	0.305
HLA2	-0.685	-0.410	-0.844
HLA3	-0.674	-0.123	0.751
HLA4	-0.038	0.599	-0.689
HLA5	-0.692	-0.410	0.560
HLA6	0.335	0.230	-1.032
HLA7	0.315	-0.522	-0.041
HLA8	0.599	0.112	0.108
HLA9	-0.175	-0.570	0.705
HLA10	0.095	0.495	0.038
HLA11	0.039	-0.672	0.458
HLA12	-0.164	-0.410	-0.156
HLA13	0.105	-0.263	-0.163
HLA14	0.898	0.943	0.074
HLA15	-0.165	-0.481	0.728
HLA16	-0.123	-0.005	-0.173
HLA17	0.365	0.111	-0.282

C. Connecting weight (AxB)

	HLB1	HLB2	HLB3
I1	0.483	-1.431	-0.514
I2	0.495	-0.138	-2.237
I3	0.418	-1.183	0.861
I4	-0.436	-2.578	-0.656
I5	2.171	-0.340	0.612
I6	0.397	-1.370	2.338
I7	-0.258	0.274	2.143
I8	0.004	-0.704	0.116
I9	-0.315	0.144	1.074

Weights (CxD)	Rank	Normalized weights
2.230	6	0.894
2.768	4	1.109
3.491	3	1.399
4.862	2	1.948
0.692	9	0.277
5.799	1	2.323
2.264	5	0.907
1.661	7	0.665
1.192	8	0.478

D. OUTPUT LAYER (OL) Weights.

OL1	OL2	OL3
-0.380	-2.149	1.285

ANN Derived weights

Ranks	6	4	3	2	9	1	5	7	8
Weights	0.893517	1.108927	1.39864	1.948046	0.277402	2.323309	0.907107	0.665373	0.477588
Layers	Lineament	Slope amount	Road zone	lithology	landuse	Mass wasting	vegetation	drainage	aspect

References

[1] FOGEL, D. B., WASSON E.C, BOUGHTON, E.M, PORTO, V.W., 1998, Evolving artificial neural networks for screening features from mammograms. Artificial Intelligence in Medicine, 14, pp. 317 - 326.

[2] PRADHAN, B., MANSOR, S., LEE, S. AND BUCHROITHNER, M. F., 2008, Application of a data mining model for landslide hazard mapping. International Archives of the photogrammetry, remote sensing and spatial information sciences, 37, pp. 187 - 196.

[3] LEE, S AND EVANGELISTA, D.G., 2006, Earthquake-induced landslide susceptibility mapping using an artificial neural network. Natural Hazard Earth System Science, 6, pp. 687 - 695.

[4] GOMEZ, H. AND KAVZOGLU, T., 2005, Assessment of shallow landslide susceptibility using Artificial Neural Network in Jabonosa River Basin, Venezuela. Engineering Geology, 78, pp. 11 - 27.

[5] ERCANOGLU, M. AND GOKCEOGLU, C., 2002, Assessment of landslide susceptibility for a landslide-prone area (north of Yenice, NW Turkye) by fuzzy approach. Environmental Geology, 41, pp. 720 - 730.

[6] PISTOCCHI, A., LUZI, L. AND NAPOLITANO, P., 2002, The use of predictive modeling techniques for optimal exploitation of spatial databases: a case study in landslide hazard mapping with expert system-like methods. Environmental Geology, 41, pp. 765 - 775.

[7] LEE, S., RYU, J. H., MIN, K. AND WON, J. S., 2003, Landslide susceptibility analysis using GIS and artificial neural network, Earth Surface Processes and Landforms, 27, pp. 1361 - 1376.

[8] ARORA, M. K., DAS GUPTA, A. S. AND GUPTA R. P., 2004, An Artificial Neural Network approach for landslide hazard zonation in the Bhagirathi (Ganga) valley, Himalayas. International Journal of Remote Sensing, 25, pp. 559 - 572.

[9] KANUNGO, D. P., ARORA, M. K., SARKAR, S. AND GUPTA, R. P., 2006, A comparative study of conventional, ANN black box, fuzzy and combined neural and fuzzy weighting procedures for landslide susceptibility zonation in Darjeeling Himalayas. Engineering Geology, 85, pp. 347 - 366.

[10] ERMINI, L., CATANI, F. AND CASAGLI, N., 2005, Artificial Neural Network to landslide Susceptibility assessment. Geomophology, 66, pp. 327 - 343

[11] RAUTELA P. AND LAKHERA, R.C., 2000, Landslide risk analysis between Giri and Tons Rivers in Himachal Himalaya (India). Journal of Applied Geomorphology, 2, pp. 153 - 160

[12] TZENG, F. Y AND MA, K. L., 2005, Opening the black box- data driven visualization of neural network. In: Proceedings of the 16th IEEE visualization, pp. 49

[13] LINGIREDDY, S. AND BRION, G.M., 2005, Artificial Neural Networks in Water Supply Engineering. A Task Committee Report on Artificial Neural Network Applications in Water Supply Engineering, Eds. Lingireddy and Brion, American Society of Civil Engineers (ASCE).

[14] PRINCIPE, J., EULIANO, N. AND LEFEBVRE, W., 2000, Neural and Adaptive Systems: Fundamentals through Simulations. John Wiley & Sons, New York

[15] MCCULLOCH, W. S. AND PITTS, W., 1943, A logical calculation in the ideas imminent in nervous activity. Bulletin of Mathematical Biophysics, 5, pp. 115 - 133.

[16] HOPFIELD, J. J., 1982, Neural network and physical systems with emergent collective computational abilities. Proceedings of the National Academy of Sciences, USA, 79, pp. 2554 - 2558.

[17] HAYKIN, S. (Ed), 1999, Neural Networks: A comprehensive foundation. New Jersey: Prentice Hall.

[18] KING, S. L., 2003, Using ROC curves to compare neural networks and logistic regression for modeling individual noncatastrophic tree mortality. In: Van Sambee, J. W., Dawson, J. O., Ponder Jr., F., Loewenstein, E. F., Fralish, J. S., (Ed.), Proceedings of the 13th Central Hardwood Forest Conference; Gen. Tech. Rep. NC-234. St. Paul, MN: U.S. Department of Agriculture, Forest Service, North Central Research Station, pp. 349 - 358.

[19] GURCAN, M. N., SAHINER, B., CHAN, H. P., HADJIISKI, L. AND PETRICK, N., 2000, Optimal selection of neural network architecture for CAD using simulated annealing. Engineering in Medicine and Biology Society. Proceedings of the 22nd Annual International Conference of the IEEE, 4, pp. 3052 - 3055.